The Qualitative Analysis of Nonlinear Parameterised Systems

Part II

A Method for the Global Analysis of Nonlinear Systems

B.R. Haynes †

S.A. Billings ††

† Department of Electronic and Electrical Engineering

University of Leeds

Leeds LS2 9JT, U.K.

†† Department of Control Engineering

University of Sheffield

Sheffield S1 3JD, U.K.

Research Report No. 400

August 1990

The Qualitative Analysis of Nonlinear Parameterised Systems

Part II - A Method for the Global Analysis of Nonlinear Systems

Abstract

In Part I of this paper the representation of nonlinear systems, and results from dynamical systems were introduced. In this, the second part, a method for the global analysis of nonlinear systems is presented.

Several examples are used to illustrate the type of results that can be achieved using the new approach. It is shown that all typical bifurcation phenomena can be detected. A nonlinear feedback system is also analysed in order to show how the new approach provides both qualitative information and a global perspective over a defined region of the systems parameter space. The method proves to be a powerful tool when used to probe the nonlinear characteristic of a system.

Introduction

In Part I of this paper we reviewed the representation of a variety of nonlinear model types. In general the method of analysis for such models depends primarily on the model structure. One approach, which can be placed under the broad heading of dynamical systems theory, is particularly attractive. In Part I we reviewed the basis of this theory and the main results.

Unfortunately, the analytical based methods rely on detailed a priori knowledge of the nonlinear models solution structure, before they can be applied. In essence they require the analyst to know where the interesting behaviour lies in the product of the problems state space and parameter space, before he can analyse what type of behaviour is occurring. In practice this means being able to characterise the solution structure of the nonlinear equations describing the system over some region of the state space for a given range of parameters.

In this paper we get around this problem by adopting a particularly attractive numerically based method, the *cell map* algorithm. This algorithm is first extended to allow the analysis of the type of parameterised nonlinear problems discussed in Part I. This simple approach is applicable to a diverse range of model structures. In addition it provides a global aspect to the analysis which is very difficult to achieve using previous analytical or numerical approaches.

A number of simple examples are used to illustrate how typical bifurcation phenomena can be detected along with almost complete characterisation of the systems local and global stability over a defined region. Finally, a nonlinear feedback system is analysed to illustrate the flexibility and ease of use involved in parameterising a nonlinear problem and suspending it in the cell map framework.

parameter μ. A predictor corrector method is typically used. Differentiation of $\mathbf{g}(\mathbf{x}(\mu),\mu)$ with respect to μ gives

$$\mathbf{g}_x \frac{\partial \mathbf{x}}{\partial \mu} + \mathbf{g}_\mu = 0 \tag{1.3}$$

where $\mathbf{g}_\mu$ denotes the n vector with components

$$\mathbf{g}_\mu(\mathbf{x},\mu) = \left(\frac{\partial g_1}{\partial \mu}, \ldots, \frac{\partial g_n}{\partial \mu} \right)^T \tag{1.4}$$

Rearranging and evaluating about $\mathbf{x}_0,\mu_0$ gives

$$\frac{\partial \mathbf{x}}{\partial \mu}(\mathbf{x}_0,\mu_0) = -\left(\mathbf{g}_x^0\right)^{-1} \mathbf{g}_\mu^0 \tag{1.5}$$

where $\mathbf{g}_\mathbf{x}^0 = \mathbf{g}_x\,(\,\mathbf{x}_0,\mu_0\,)$ and $\mathbf{g}_\mu^0 = \mathbf{g}_\mu\,(\,\mathbf{x}_0,\mu_0\,)$. A Euler predictor approximation to $\mathbf{x}(\mu_0+\Delta\mu)$ is then given by

$$\mathbf{x}^p = \mathbf{x}_0 + \Delta\mu \left(\frac{\partial \mathbf{x}}{\partial \mu} \right)_0 \tag{1.6}$$

which is used as a starting value to solve the system.

$$\mathbf{g}\,(\,\mathbf{x}\,,\,\mu+\Delta\mu\,) = 0 \tag{1.7}$$

This simple procedure is then called an Euler-Newton continuation method [Keller, 1977]. The method works well and forms the basis of many computer codes.

The path following method runs into trouble at points where $\mathbf{g}_\mathbf{x}^0$ is singular, in particular if the path $\mathbf{x}(\mu)$ bends back upon itself, as in Fig. (0) at μ_c, the method then fails. Addition of an auxiliary equation to (1.2) is often used to circumvent this difficulty [Keller, 1977, Doedel, 1981, Hente and Jansen, 1986].

Many implementations of the above algorithm are in existence. Codes such as PITCON, [Rheinboldt et al, 1978, 1983, 1986], AUTO, [Doedel, 1981, 1986] and PATH, [Kass-Petersen, 1987a, 1987b] proceed in a tangential direction adjusting the step length in this fixed direction in order to obtain a new predicted point near the solution arc. Mittlemann, 1986, presents a method to overcome the problem of very small step sizes produced by sharp curves.

The code BISTAB, [Wood et al, 1984], computes bifurcation curves of equilibrium solutions of (1.1) as any one of 10 parameters are varied. The code determines the stability of branches and detects Hopf points by monitoring the Jacobian. The code uses the continuation method of

Kubicek, 1976, and Keller, 1977.

The code BIFOR2, [Hassard et al, 1980] computes Hopf points of an ODE's and determines the direction and stability of the periodic solution. More recently the code HOPFDR, [Roose, 1987, and Roose and Deir, 1987], provides a direct method for the computation of Hopf points near a turning point and improves on the method used in BIFOR2.

Finally the codes AUTO, [Doedel, 1981, 1986], and BIFPACK, [Seydel, 1979a, 1979b, 1983a and 1983b] compute bifurcations and continue branches, determining stability in both the equilibrium and periodic solutions of (1.1) [Brindley et al, 1989].

The general parameter dependent nonlinear equation in many applications, see for instance the references cited in Part I. Under natural conditions on **f** the set of solutions of (1.2) constitutes a differentiable manifold in the product of state space and parameter space. The dimension of this manifold equals that of the parameter space.

Unfortunately the available path following methods provide information on only the local stationary solutions of ODE's. And once again, as in the analytical approach, a priori knowledge is needed. One or more points on a known solution branch must be provided in order to start tracing the solution arc. In order to detect any splitting or bifurcation points an additional *branch switching* algorithm must be employed. Furthermore, no information is provided on the extent of the influence domains, or DOA, of the branches traced out. No account is taken of the possibility of disjoint or isolated solution arcs existing.

In most practical applications attention centers not so much on computing a few solutions but rather in determining the form and special features of the solution manifold. At present the standard computational methods for such analysis require the user to construct a picture of a p-dimensional manifold from information along a 1-dimensional path [Rheinboldt, 1988]. In general this is not easy to achieve and can lead to misinterpretation of the solution structure. A method which allows a more complete approach to the problem is required. In order to overcome these short comings we adopt an entirely different algorithmic approach which we discuss next.

The method of *Cell-to-Cell* mapping, [Hsu and Guttalu, 1980, Hsu, 1981, 1982, Hsu, Guttalu and Zhu, 1982], provides one possible solution which offers both qualitative results and global stability information with little need for a priori information. Adopting this algorithm and subsequently extending it to the analysis of a general parameterised systems provides an extremely flexible tool for analysis. Implementation of the extended cell map algorithm on an interactive graphical

workstation provides a versatile tool for studying nonlinear systems within the framework of ideas discussed in Part II. Next we describe the basis of this essentially algorithmic approach. The method, being intrinsically computational, leads to the development of an algorithmic framework. For a more recent and complete overview of the theory see Hsu, 1987 and the references cited therein.

1.1. Cell-to-Cell Mappings

In the conventional setting consider the state space **X** of a dynamical system to be a continuum of dimension n. The basic idea behind the cell mapping method is to consider the state space, not as a continuum, but rather as a collection of a large number of cells, with each cell an entity in the state space. Before describing the method a number of definitions are required.

Define - a *cell state space,* $\mathbf{Z}^n$, as an n-dimensional space whose elements are n-tuples of integers. Each element is called a *cell vector,* or simply a *cell*, and is denoted by **z**.

There are many ways to obtain a cell structure over a given euclidean state space. The simplest way is to construct a cell structure consisting of rectangular parallelepipeds of uniform size (squares, cubes etc). Let x_i ,$i = 1,..,n$ be the state variables and let each coordinate axis of the state variable be divided into a number N_i, of intervals of uniform size h_i. The interval z_i along the x_i axis is defined such that it covers all the x_i of interest.

$$(z_i - \frac{1}{2}) h_i \le x_i \le (z_i + \frac{1}{2}) h_i \qquad z_i = 1,2,..,N_i \tag{1.8}$$

The n-tuple z_i ,$i = 1,..,n$ is then called the cell vector, denoted by **z**. A point **x** with components x_i ,$i = 1,..,n$ belongs to a cell **z** with components z_i ,$i = 1,..,n$ if and only if x_i and z_i satisfy (1.8) for all $i \in [1,n]$. Within this cell state space the simple Cell Mapping is then defined by

$$\mathbf{z}(j+1) = \mathbf{C}(\mathbf{z}(j)) \qquad \mathbf{z}(j) \in \mathbf{Z}^n \subset \mathbf{S} \tag{1.9}$$

Define - the *cell map,* **C(z)**, as a mapping of a set if integers $\{N+\}$ to a set of integers $\{N+\}$, where $\{N+\} = \{0,1,..,N\}$.

Define - the *unit vectors,* $\mathbf{e}_j$, $j \in [1,n]$ as $\mathbf{e}_j = (0,0,..,0,1,0,..,0)^T$, $\forall j = 1,..,n$.

Define - two cells **z** and **z'** to be *adjoining* if and only if $\underset{1 \le j \le n}{Max} \mid \mathbf{z} - \mathbf{z}' \mid = 1$

Define - two cells to be *contiguous* if and only if $\mathbf{z} - \mathbf{z}' = \pm \mathbf{e}_j$ for some $j \in [1,n]$.

Define - the *cell function*, $\mathbf{F}(\mathbf{z},\mathbf{C})$, as

$$\mathbf{F}(\mathbf{z},\mathbf{C}) = \mathbf{C}(\mathbf{z}) - \mathbf{z} \tag{1.10}$$

and the k-th step ahead *cell function* as

$$\mathbf{F}(\mathbf{z},\mathbf{C}^k) = \mathbf{C}^k(\mathbf{z}) - \mathbf{z} \tag{1.11}$$

where $\mathbf{C}^k(\mathbf{z})$ denotes $\mathbf{C}(\mathbf{z})$ applied k times.

Define - the *singular cell* as a cell $\mathbf{z}^*$ satisfying the relationship

$$\mathbf{F}(\mathbf{z}^*,\mathbf{C}) = 0 \qquad \text{and} \qquad \mathbf{z}^* = \mathbf{C}(\mathbf{z}^*) \tag{1.12}$$

A *solitary singular* cell is a singular cell with no contiguous singular cells. A *core* of singular cells is a singular cell with a complete set of contiguous cells that are also singular.

Define - a *periodic cell*, given that $\mathbf{C}^k(\mathbf{z})$ denotes $\mathbf{C}(\mathbf{z})$ applied k times with $\mathbf{C}^0(\mathbf{z})$ understood to be the identity mapping, as a member of the sequence $\mathbf{z}^*(j)$, $j = 1,..,k$ which satisfies

$$\mathbf{z}^*(j+1) = \mathbf{C}^j(\mathbf{z}^*(1)) \qquad j = 1,..,k-1 \qquad \mathbf{z}^*(1) = \mathbf{C}^k(\mathbf{z}^*(1)) \tag{1.13}$$

The above constitutes a periodic motion of period k, that is a **P-K** cycle. Each element of the cycle is a **P-K** cell. It is readily seen that a **P-K** cycle is a singular cell of the k-step cell function

$$\mathbf{F}^k(\mathbf{z}^*,\mathbf{C}^k) = 0 \tag{1.14}$$

The concept of an influence domain or domain of attraction has a very simple interpretation in the cell state space around a periodic or singular entity. A cell $\mathbf{z}$ is said to be r-steps removed from a **P-K** cycle if r is the minimum positive integer such that $\mathbf{C}^r(\mathbf{z})=\mathbf{z}^*(j)$ where $\mathbf{z}^*(j)$ is one of the **P-K** cells within the **P-K** cycle.

Define - the r-step *domain of attraction* as the set of all cells which are r-steps or less removed from a particular **P-K** solution.

Define - the *total domain of attraction* as the r-step domain of attraction with $r \to \infty$.

The domain then covers all cells within the influence of this cycle. Hence forth we refer to this as simply the *domain of attraction*, or **DOA**, of the cycle.

Define - the *domain of attraction of all* **P-K** cycles, that is the **DOA-K**, as the set of all cells within the influence domain of any and all **P-K** cycles, where k is fixed.

This definition becomes especially useful when differentiating between the stable attracting equilibria, or **P-1** fixed points, and the stable attracting orbits, or **P-K** cycles.

For most practical systems there are ranges of values of the state variable beyond which we are no longer interested. This means that there is only a finite region of the state space which is of concern. Similarly for a dynamical system governed by a cell mapping there is only a finite region of the cell space in which we are interested, and correspondingly a finite number of cells, named the *regular cells* totalling N_c in number. This allows the introduction of a ***sink cell*** which is used to encompasses all possible cells outside the region of interest. If the mapped image of a regular cell lies outside the region of interest it is then said to be mapped into the sink cell.

The regular cells are labelled by positive integers $\{1,2..,N_c\}$. The sink cell is labelled as the zero, $\{0\}$, cell. This makes the total number of cells in the cell state space N_c+1, such that $\mathbf{S}=\{N_c+\}$. The set is closed under the mapping described by

$$\begin{aligned} \mathbf{z}(j+1) &= \mathbf{C}(\mathbf{z}(j)) & \mathbf{z}(j),\ \mathbf{z}(j+1) &\in \mathbf{Z}^n \subset \mathbf{S} \\ \mathbf{C}(0) &= 0 & \mathbf{S} &= \{N_c+\} \end{aligned} \tag{1.15}$$

A number of interesting consequences arise from the nature of the cell state space and the definitions above. The sink cell, **C**(0), is a **P-1** cell and we can denote the set of regular cells within the influence domain of the sink cell, that are being eventually mapped to **C**(0), as being in the domain of attraction of the sink cell. These cells are known as the **DOA-Sink** cells. Such cells may form part of the unstable domain of the cell state space, they may however just form a demarcation between cells invariant to the region of interest chosen and those that are mapped outside the region of interest. Care must then be taken with the interpretation of the sink cell as representing the unstable region of the cell state space. The number of periodic cells may be very large. It may not however exceed N_c. Likewise **P-K** periodic cycles can have various periods, but must satisfy $\mathbf{K}\leq N_c$.

The evolution of a Cell Map (1.15) starting at a regular cell $\mathbf{z}\in\mathbf{S}$ can lead to only three possibilities.

i) **z** is a periodic cell of a **P-K** cycle, the motion then follows that of the **P-K** cycle.

ii) **z** is mapped into the sink cell after *r*-steps, the cell is then in the domain of attraction of the sink cell, and is labelled as in the **DOA-Sink**.

iii) **z** is mapped into a periodic cell of a **P-K** cycle after *r*-steps, the cell is then in the domain of attraction of a periodic cycle, and is labelled as in the **DOA-K**.

1.2. Cell Mapping Discretisation

The Cell Map system may be considered simply as a discretisation of the point mapping system represented by

$$\mathbf{x}_{k+1} = \mathbf{g}(\mathbf{x}_k) \qquad \mathbf{x} \in \mathbf{R}^n \tag{1.16}$$

In order to make use of the qualitative ideas provided by the framework of dynamical systems adopted in Part I it is necessary to extend the algorithm of Hsu, 1980e.

Consider the more general parameterised nonlinear system described by

$$\mathbf{x}_{k+1} = \mathbf{g}(\mathbf{x}_k, \mu) \qquad \mathbf{x} \in \mathbf{R}^n \quad \mu \in \mathbf{R}^m \tag{1.17}$$

Applying the center point method of discretisation requires the division of the state space $\mathbf{R}^n$ into a collection of cells according to (1.8) and the calculation of the center point $\mathbf{x}^{(d)}(n)$ of $\mathbf{z}(n)$ such that

$$x_i^{(d)}(j) = h_i z_i(j) \qquad j = 1,..,N_i \quad i = 1,..,n \tag{1.18}$$

where z_i is the i-th component of $\mathbf{z}$, x_i is the i-th component of $\mathbf{x}$ and h_i is the cell size along x_i coordinate axis.

Given the lower and upper bounds to the region of interest, such that

$$\mathbf{x}^{(l)} \le \mathbf{x} \le \mathbf{x}^{(h)} \qquad \mathbf{x}^{(l)} = (x_1^{(l)},..,x_n^{(l)}) \quad \mathbf{x}^{(h)} = (x_1^{(h)},..,x_n^{(h)}) \tag{1.19}$$

the center point of each cell $\mathbf{x}$ may be calculated using

$$\begin{aligned} x_i^{(d)}(j+1) &= x_i^{(d)}(j) + h_i \qquad && i = 1,..,n \quad j = 1,..,N_i - 1 \\ x_i^{(d)}(1) &= x_i^{(l)} + \frac{h_i}{2} \qquad && \mathbf{x}^{(d)} = (x_1^{(d)},..,x_n^{(d)}) \end{aligned} \tag{1.20}$$

Taking into account the parameter vector in (1.17), having lower and upper bounds

$$\mu^{(l)} \le \mu \le \mu^{(h)} \qquad \mu^{(l)} = (\mu_1^{(l)},..,\mu_m^{(l)}) \quad \mu^{(h)} = (\mu_1^{(h)},..,\mu_m^{(h)}) \tag{1.21}$$

gives

$$\begin{aligned} \mu_i^{(d)}(j+1) &= \mu_i^{(d)}(j) + h_i \qquad && i = 1,..,m \quad j = 1,..,N_i - 1 \\ \mu_i^{(d)}(1) &= \mu_i^{(l)} + \frac{g_i}{2} \qquad && \mu^{(d)} = (\mu_1^{(d)},..,\mu_n^{(d)}) \end{aligned} \tag{1.22}$$

where g_i is the cell size along the μ_i coordinate axis such that

$$(z_i - \frac{1}{2}) g_i \le \mu_i \le (z_i + \frac{1}{2}) g_i \qquad i = n+1,..,n+m \tag{1.23}$$

The point mapping or image of the center point $\mathbf{x}^{(d)}(n)$ is then calculated using (1.17)

$$\mathbf{x}_{k+1}^{(d)} = \mathbf{g}\left(\mathbf{x}_k^{(d)}, \mu^{(d)}\right) \tag{1.24}$$

and the cell map system is constructed using

$$C_i(z_i(j)) = z_i(j+1) = \mathrm{INT}\left[\frac{\mathbf{x}_i^{(d)}(k+1) - \mathbf{x}_i^{(l)}}{h_i} + 1\right] \qquad i = 1,..,n$$

$$C_i(z_i(j)) = z_i(j) \qquad i = n+1,..,n+m \quad j = 1,..,N_i \tag{1.25}$$

Note we are in effect constructing m separate cell mappings, of dimension n each representing a slice within the parameter space $\mu = (\mu_1,..,\mu_m)^T$.

A similar approach to the construction of the cell map system may be taken for a continuous nonlinear model. Consider the creation of a cell mapping system (1.25) from the system described by

$$\dot{\mathbf{x}}(t) = \mathbf{f}(\mathbf{x}(t), \mu) \qquad \mathbf{x} \in \mathbf{R}^n \quad \mu \in \mathbf{R}^m \tag{1.26}$$

It is straight forward to create a point mapping from (1.26). Choosing a time interval τ, take an arbitrary point within $\mathbf{x} \in \mathbf{R}^n$, fix values for the parameters $\mu \in \mathbf{R}^m$, and calculate the resulting trajectory for $t = 0 - \tau$.

This method can then be used to approximate the mapping image of the center points $\mathbf{x}_{k+1}^{(d)}$, $\mu_{k+1}^{(d)}$ in (1.20-25). All that is required is a suitable integration scheme to solve

$$\mathbf{x}_{k+1}^{(d)} = \mathbf{x}(\tau)^{(d)} = \mathbf{x}(0)^{(d)} + \int_0^{\tau} \mathbf{f}\left(\mathbf{x}(t), \mu^{(d)}\right) dt \tag{1.27}$$

The only additional information required is the time step τ and an integration interval T. T is chosen as would be normal for the problem, bearing in mind the choice of integration method. τ is dependent on the cell size and should be chosen such that image of the center point of a cell lies within a neighbouring cell. This obviously depends upon the strength of the local vector field and will vary from cell to cell throughout the entire cell space. If the interior of the cell contains an attracting equilibria, the trajectory described by (1.40) will remain within that cell. An interactive approach to the choice of τ is best adopted. Generally choosing τ to be 3-15 times the integration interval T gives good results.

1.3. Global Characteristics of the Cell Map

In its basic form the cell map approach is very simple. It is this simplicity that makes it applicable to a wide range of nonlinear problems. Little *a priori* knowledge is required. In addition the analysis provides a global picture of the system characteristics that are difficult to obtain by other means.

In order to describe this method of global analysis, called the *Global Unravelling* algorithm [Hsu, 1987], it is necessary to delineate the global properties of each cell $\mathbf{z} \subset \mathbf{S}$ by specifying just two numbers :-

i) Group number $g_r(\mathbf{z})$

To each existing periodic cycle assign a *group number* g_r. This number is used as an identification tag and is given to every periodic cell in that cycle and also to every cell in the domain of attraction of that cycle. Each group has, as its invariant set, that **P-K** cycle. Obviously there will be as many groups as there are periodic motions. The total number of groups is denoted by n_{gr}.

ii) Period number $p_d(\mathbf{z})$

To each cell in the group $g_r(j)$ a periodicity is assigned. If a cell has a periodicity $p_d(j)=k$ then that cell is a member of a **P-K** cycle. If a cell has a periodicity $p_d(j)=-k$ then that cell is in the domain of attraction of the **P-K** cycle.

Note these definitions differ slightly from those used in Hsu and Guttalu, 1980.

1.4. Suspended Cell Map System

The *Unravelling* algorithm can be made to work most computationally efficiently on 1-dimensional cell maps which are of the form

$$z(j+1) = \mathbf{C}(z(j)) \qquad z(j), z(j+1) \in \mathbf{Z}^1 \subset \mathbf{S} \tag{1.28}$$

The general $n+m$-dimensional parameterised bifurcation problem, (2.1) or (2.7) in Part I, is now considered as *suspended* within a cell map framework. This means the mapping

$$\mathbf{x}_{k+1} = \mathbf{g}(\mathbf{x}_k, \mu) \qquad \mathbf{x} \in \mathbf{R}^n \quad \mu \in \mathbf{R}^m \tag{1.29}$$

becomes

$$\mathbf{z} = \mathbf{C}(\mathbf{z}) \qquad \mathbf{z} = (\mathbf{z}, \mu)^T \quad \mathbf{z} \in \mathbf{Z}^{n+m} \tag{1.30}$$

where the increase in the dimension of the cell state space reflects the parameterisation of the problem. The $n+m$ dimensional cell map is then transformed to a 1-dimensional Map using

$$z = z_1 + (z_2-1)N_1 + (z_2-1)(z_3-1)N_2 + \cdots$$

$$C = C_1 + (C_2-1)N_1 + (C_2-1)(C_3-1)N_2 + \cdots \qquad (1.31)$$

Such a transformation has no effect on the dynamics of the cell map, but merely results in a re-labelling of the cells.

1.5. Global Unravelling Algorithm

The algorithm as it stands enables the determination in one computer run, all of the periodic cells and their respective domains of attraction, in **S**. It involves essentially calling up each cell in the set **S** and processing it in order to determine its global characteristics which are then assigned using g_r and p_d. At initialisation all cells have $g_r(z)$ and $p_d(z)$, set to zero, $\forall z \in \mathbf{S}$. The algorithm distinguishes between three different types of cell

i) Cells which have not yet been processed are called *virgin* cells, for which $g_r(z)=0$.

ii) Cells which are currently being processed, the *current* cells, for which $g_r(z)=-1$.

iii) Cells which have been processed and whose global properties are known are called *processed* cells and are distinguished by $g_r(z)\geq 1$.

The processing of the cells repeatedly makes use of the m-th order cell processing sequence starting at a base cell b

$$b \rightarrow \mathbf{C}(b) \rightarrow \mathbf{C}^2(b) \rightarrow \cdots \rightarrow \mathbf{C}^{m-1}(b) \rightarrow \mathbf{C}^m(b) \qquad (1.32)$$

In the algorithm the cells are processed in a sequential order taking b successively as

$$b = j = 0, 1, 2, .., N_c \qquad \forall z \subset \mathbf{S} \qquad (1.33)$$

The algorithm takes each cell b in (1.33), which is a virgin cell, as a base cell. At each stage in the sequence (1.32) three possibilities occur

i) The new cell $\mathbf{C}^m(b)$ is such that $g_r(b)>0$

The new cell is then found to be part of a previous sequence and hence all its global characteristics are already known. All the cells in the current processing sequence inherit the same group number and periodicity as $\mathbf{C}^m(b)$. The algorithm then moves on to the next cell in (1.33).

ii) The new cell $\mathbf{C}^m(b)$ is such that $g_r(b) = -1$

This indicates that the new cell has then appeared before in the current processing sequence and hence there is a periodic motion contained within the current sequence (1.32). Moreover this **P-K** cycle is a new one. To all cells in the sequence a new group number is assigned. It is then a simple matter to iterate once more around the cycle to detect its period **P-K** and to set the group number and periodicity of the cycle. The rest of the current sequence is labelled as in the same group but the periodicity is set negative to indicate the cells make up part of the **DOA** of a **P-K** cycle.

iii) The new cell $\mathbf{C}^m(b)$ is such that $g_r(b) = 0$

If this condition holds the next cell in the sequence is also a virgin cell and so the current sequence must be mapped once more according to (1.32). The unravelling algorithm then returns to stage i).

Notice that the first processing sequence begins with the sink cell, $z = 0$, which becomes $\mathbf{C}(0) = 0$, and is therefore a **P-1** cell, where $g_r(0) = 1$ and $p_d(0) = 1$.

The advantage of the above approach is that it combines the qualitative aspects of a dynamical systems theory with the global aspect afforded by the Global Unravelling algorithm. In implementing the above algorithm many variations are possible. The version developed in this work focuses on the problems of enumerating the global characteristics of the parameterised problems discussed in Part I of this paper. One aim throughout this work has been to maintain an interactive aspect to the algorithm. This enables the analyst to probe the dynamics of a problem in an interactive manner by varying the extent of the cell state space. In order to achieve this, a fast speed of execution of the algorithm is of prime importance. There is a considerable computational burden in the construction of the Cell Map using (1.17-25) and (1.26-27). This may be reduced by careful consideration of the manner in which vector and matrix operations are executed.

Examples

2.0. Introduction

The first of these examples illustrates that the approach of suspending a parameterised nonlinear model in the cell map framework, does indeed produce the type of qualitative information to be expected from a bifurcation study.

Example 1 Saddle Node Normal Form

The normal form for the saddle node bifurcation for a 1-parameter family is

$$\dot{x}(t) = \mu - x^2 \tag{2.1}$$

Suspending this ODE in the parameterised cell map framework above yields the cell system

$$z = \mathbf{C}(z,\mu) \qquad z \in \mathbf{Z}^1 \quad \mu \in \mathbf{Z}^1 \tag{2.2}$$

Defining the cell state space **C** such that $z_1 \in [-1,1]$ and $z_2 \in [-1,1]$ over a mesh of 200×200 cells and using a 4-th order Runge-Kutter method with integration step $T = 0.1$ and $\tau = 0.5$, results, on application of the unravelling algorithm, in the cell map diagram Fig. (1).

Comparison with Fig. (1), in Part I of this paper, reveals that the global analysis approach has successfully captured the complete characteristic associated with the saddle node. A smooth curve of **P-1** cells delineate the familiar saddle node form. In addition essential global stability information is also provided. The shaded area delineates the sink cell, that is the unstable region. Furthermore, stability information on the curve of **P-1** cells provides an indication as to the local behaviour of the curve of fixed points detected. The lower section of this curve is made up of unstable equilibria representing the saddle points in the bifurcation.

Example 2 Transcritical Normal Form

The normal form for the transcritical bifurcation is given by

$$\dot{x}(t) = \mu x - x^2 \tag{2.3}$$

Defining the cell state space as above and applying the unravelling algorithm results in the cell map diagram, Fig. (2). Again the algorithm has successfully detected the expected characteristic, see Fig. (2), in Part I. Global and local stability information provided by the **DOA-Sink**, which

indicates that the trivial equilibrium along $x = 0$ to be stable for $\mu < 0$ and unstable for $\mu > 0$.

Example 3 Pitchfork Normal Form

The normal form for the pitchfork bifurcation is given by

$$\dot{x}(t) = \mu x - x^3 \tag{2.4}$$

Repeating the above exercise as above once more results in the cell map diagram, Fig. (3). Again the global analysis approach has successfully captured the characteristic pitchfork bifurcation, see Fig. (3), in Part I. Notice that this time the entire cell space is stable. This means that the influence of the sink cell is zero because all cells are in the **DOA** of one or other stable fixed points or **P-1** cells.

In this case the bifurcation point at the origin $(x, \mu) = (0,0)$ is detected by a core or blob of **P-1** cells. The core can be reduced in size by more careful choice of the time intervals T and τ. Alternatively increasing or decreasing the number of cells will improve the resolution of the results obtained about any point of particular interest. The amount of computational effort directed towards this problem depends largely on the level of accuracy deemed necessary for a particular system.

The proceeding examples illustrate the success of the approach as applied to simple parameterised ODE's. The inherent flexibility of the method means it can equally well be applied to maps.

Example 4 Flip Normal Form

The normal form for the flip period doubling bifurcation for maps is given by

$$x_{n+1} = -(1+\mu)x_n + x_n^3 \tag{2.5}$$

This model is an autonomous form of the NARMAX model, see Part I of this paper. Suspending (2.5) in the cell map framework and defining the cell state space as $z_1 \in [-1,1]$ and $z_2 \in [-1,1]$ over a mesh of 200×200 results in the Cell diagram, Fig. (4). Again the parameterised algorithm has successfully captured the expected characteristic, see Fig. (5), in Part I. The nontrivial equilibria being a period 2 cycle, is detected as a **P-2** cell cycle.

Example 5 Incomplete Cascade to Chaos

As a illustration of the algorithms ability to detect higher order **P-K** cycles the unravelling algorithm was applied to the system described by [Thompson and Stewart, 1986]

$$x(k) = \mu + \frac{\alpha x(k-1)}{1 + x^2(k-1)} \tag{2.6}$$

Note how this model takes the form of a rational difference equation. Fortunately this change of model structure presents no problem to the cell map approach. In this example the parameters μ and α may be considered as either input terms of system parameters. In this case taking $\alpha = 11.5$ and suspending the system in the cell state space $z_1 \in [0,5]$ and $z_2 \in [-5,0]$ over a grid 750×750 cells. Applying the unravelling algorithm results in the cell map diagram, Fig. (5). The first plot shows the so called incomplete cascade to chaos, a sequence of flip, period doubling, bifurcations **P-2** to **P-8**. The somewhat larger number of cells chosen in this example was to pick out the detail near the **P-8** points whilst at the same time maintain the global picture of the characteristic. The second plot reveals the **P-1**, **P-2**, **P-4** and **P-8** cell cycles individually and the lower plot completes the picture by including the **DOA** of the unstable sink cell. Notice how the global aspect of the cell map approach reveals a complete picture of the qualitative characteristic for this system. Both the periodic behaviour and local and global stability information are provided in one step.

Example 6 Hahn Feedback System

In a nonlinear system the type of bifurcation characteristic obtained depends largely on the bifurcational parameter selected. In real problems, where there may be a number of parameters of interest, the selection of a *primary parameter* may become critical. One parameter may well form the dominant characteristic, on the other hand, two or more parameters may interact strongly, requiring greater powers of analysis to be applied to the problem. As yet no really feasible numerical approach exists for problems with two or more parameters.

$$\mathbf{x}_{k+1} = F(\mathbf{x}_k, \alpha_1, \alpha_2) \qquad \mathbf{x} \in \mathbf{R}^2 \quad \alpha_{1,2} \in \mathbf{R} \tag{2.7}$$

The more rigorous methods of singularity theory, discussed earlier, consider a primary parameter, μ, along with a vector of secondary or perturbation parameter, α. The α_i contribute to form a family of perturbations in the parameter space $\mathbf{R}^k$.

$$G(\mathbf{x}_k, \mu, \alpha) \qquad \mathbf{x} \in \mathbf{R} \quad \mu \in \mathbf{R} \quad \alpha \in \mathbf{R}^k \tag{2.8}$$

The method is essentially still only 1-dimensional in the parameter.

In nonlinear studies the system input, u, has proven to be especially important. From the viewpoint of control it is often a system gain parameter that is the focus of attention.

It is possible then to apply the cell mapping approach in a 2-dimensional manner. In the following example the system set point, r, along with the feedback gain, k, are taken to be parameters. The approach adopted here is to consider two parameters selected as initially of equal importance. Of course in other problems different combinations may well be chosen.

Given a nonlinear feedback system of the form

$$\dot{\mathbf{x}}(t) = \mathbf{A}\,\mathbf{x}(t) + F(\mathbf{x}(t)) + \mathbf{B}\,\mathbf{u}(t) \qquad x\in\mathbf{R}^n \quad u\in\mathbf{R}^l \quad y\in\mathbf{R}^m \quad \mathbf{F}:\mathbf{R}^n\times\mathbf{R}^n\rightarrow\mathbf{R}^n$$

$$\mathbf{y}(t) = \mathbf{C}\,\mathbf{x}(t) \qquad \mathbf{A}: n\times n \quad \mathbf{B}: n\times l \quad \mathbf{C}: m\times n \tag{2.9}$$

applying linear state feedback

$$\mathbf{u}(t) = r - \mathbf{K}\,\mathbf{x}(t) \qquad r\in\mathbf{R}^l \quad \mathbf{K}: l\times n \tag{2.10}$$

where r is the system set point, results in the closed loop system, Fig. (6a). Setting $n=2$, $m=l=1$ results in a SISO system with 2nd order dynamics. Defining the system matrices

$$\mathbf{A} = \begin{bmatrix} 0 & -1 \\ 1 & 0 \end{bmatrix} \quad \mathbf{B} = \begin{bmatrix} 1 \\ 0 \end{bmatrix} \quad \mathbf{C} = \begin{bmatrix} 0 & 1 \end{bmatrix} \quad \mathbf{K} = \begin{bmatrix} k \\ -k \end{bmatrix} \tag{2.11}$$

and taking the nonlinear term $F(\mathbf{x})$ completes the system definition.

$$F(\mathbf{x}) = \begin{bmatrix} 2(x_1 - x_2)^3 \\ 0 \end{bmatrix} \tag{2.12}$$

The characteristic of this system is dominated by the system gain k. This is easily demonstrated by performing a set of simple step tests [Hahn, 1985]. Fig. (6b) show the step responses of the system for gains $k=0.5, 1.0, 1.25$ and 1.5. The response is dependent upon the magnitude of the gain, k, and the input set point, r. Larger gain, or large set point values, result in an oscillatory response. For $k=0.5$, and a small input, the system is attracted to the stable equilibrium at the origin. For larger input set points, unstable limit cycles surrounding the origin induce a more oscillatory response. For $k=1.0$ a similar scenario exists. System damping is at its maximum here as is the size of the DOA. At this point the stable origin undergoes a pitchfork type bifurcation. At $k=1.25$, oscillatory behaviour increases as the equilibria moves closer to the unstable limit cycles. Finally at $k=1.5$, a Hopf type bifurcation occurs resulting in two stable limit cycles placed both sides of the origin.

Such systems can be analysed directly, both *Hopf* bifurcation theory [Marsden and MaCracken, 1976] and *Describing* function methods [Hahn, 1895] have been applied with some success. However, neither method gives rise to a global picture of the system characteristic.

Cell Map Analysis $\mu = k,\ r = 0$

Consider the cell map analysis of the system, writing (2.9) in the form of the now familiar bifurcation problem gives

$$\dot{\mathbf{x}}(t) = F(\mathbf{x},\mathbf{r},\mathbf{k}) \qquad \mathbf{x}\in\mathbf{R}^2 \quad \mathbf{r}\in\mathbf{R} \quad \mathbf{k}\in\mathbf{R} \tag{2.13}$$

Selecting the primary parameter as the system gain, $\mu = k$, and setting $r = 0$ gives

$$\dot{\mathbf{x}}(t) = F(\mathbf{x},\mu) \qquad \mu = k \quad r = 0.0 \quad \mathbf{x}\in\mathbf{R}^2 \quad \mu\in\mathbf{R} \tag{2.14}$$

Suspending the system in the cell map framework by defining the cell state space, **C**, such that $Z_1\in[-1,1]$, $Z_2\in[-1,1]$ and $Z_3\in[-0,2.0]$ over a mesh of 175x175x30 cells, and applying the the *Unravelling* algorithm resulted in the Cell diagram Fig. (6c).

This diagram serves to confirm the behaviour observed in the simple step tests. For values of feedback gain k outside the range $0\leq k\leq 2.0$ the system exhibits instability. Within this range of k the shaded area of Fig. (6c) represent the stable **DOA** of a complex sequence of equilibria. The upper plots show a sequence of fixed points for $k < 1.5$. For $0\leq k\leq 1.0$ the attractor is the x-axis, at $k = 1.0$ a *Pitchfork* bifurcation takes place, the origin becoming unstable. At $k = 1.5$ a *Hopf* bifurcation results in a stable attracting limit cycle for $1.5\leq k\leq 2.0$. The lower diagrams of Fig. (6c) show this feedback induced cyclic behaviour in phase plane. For $0\leq k\leq 0.5$ the separatrix [Gumowski and Mira, 1980], marking the boundary between stable and unstable behaviour, is straddled by a number of unstable periodic cycles. It is these that produce the oscillatory characteristic seen for $k = 0.5-1.25$. Notice also that the system is open loop unstable, that is when $k = 0$.

Cell Map Analysis $\mu = r,\ k = 0.5,\ 1.0,\ 1.25$

Now taking the primary parameter to be the input set point, r, over a range of values of feedback gain $k = 0.5, 1.0$ and 1.25, the suspended problem may be rewritten as

$$\dot{\mathbf{x}}(t) = F(\mathbf{x},\mu) \qquad \mu = r \quad k = 0.5-1.25 \quad \mathbf{x}\in\mathbf{R}^2 \quad \mu\in\mathbf{R} \tag{2.15}$$

Taking $k = 0.5$ and suspending the system in the cell map framework and defining the cell state

space, C, such that $Z_1 \in [-1,1]$, $Z_2 \in [-1,1]$ and $Z_3 \in [-0.2,0.2]$, over a mesh of 175×175×30 cells, results in the Cell diagram Fig. (6d).

The upper plots show the distribution of **P-K** cycles, the shaded area represents the **DOA** of the **P-1** cycles. These vary with the input set point over the range $-0.2 \leq r \leq 0.2$. About the point $r \approx \pm 0.2$, a sequence of periodic Hopf cycles appear which mark the transition to instability. The lower phase plane plots show this *input induced* behaviour more clearly along with the **DOA** of the stable cycles. By considering the problem as essentially two dimensional in the parameter the analysis has shown the Hopf type behaviour to occur at lower values of k than was revealed by the previous analysis. In essence the the limit cycle characteristic is dependent upon both k and r.

Taking $k = 1.0$ and repeating the above analysis, results in the Cell diagram Fig. (6e). The system now has a reduced domain of stability with respect to the set point, roughly $|r| < 0.12$. For values outside this range a sequence of periodic bifurcations again lead to instability. Notice how the size of the stability domain of the periodic cycles has increased. For the larger feedback gain, the system has reduced stability with respect to its fixed point behaviour but increased internal stability in the state space, with respect to the cyclic behaviour, see Fig. (6c) and (6e).

Taking $k = 1.25$ results in the Cell diagram Fig. (6f) which further illustrates this trend. This time an unstable **P-K** cycle has been detected which marks the separatrix between the stable **DOA** and the unstable sink cells. Such high period unstable cycles are commonplace but are rather difficult to detect using path following methods.

2.1. Conclusions

The cell-to-cell mapping provides a convenient framework for the analysis of both continuous and discrete systems. Development of the suspended cell state space system, enabling an extension of the ideas to cover systems of parameterised bifurcation problems, has proved successful. The preceding examples, although simple, succeed in illustrating the concepts behind, and the use of, this approach. The qualitative approach adopted provides local and global characteristics for a wide range of systems at a level of detail appropriate to the problem.

The main problems of the algorithm are ones of visualisation and flexibility. The ultimate aim is for the development of an integrated tool for the analysis and probing of interesting dynamics within different representations of a nonlinear system. This work has gone some way to achieving this aim. There is still of course room for development, both computationally and in the

development of different algorithms to assist in the global analysis. At the moment a bifurcation is detected, or inferred to exist, simply by evidence of change in the solution structure within the cell state space.

We have contented ourselves here with the development of a tool for the global analysis of nonlinear systems. Adaptation to a form suitable for the analysis of bifurcation problems has provided a useful and more importantly, flexible methodology for the analysis of nonlinear systems.

Cell mapping have their own mathematical structure and are of considerable interest in their own right [Hsu and Leung, 1984, Hsu, 1983, Hsu and Polchai, 1984, and Hsu, 1985a]. From the theoretical point of view the methods are still in the early stages of development. This is in contrast, as we have seen, to the path following methods which are now reaching maturity both in theory and application. The method is basically then result orientated. The effectiveness of the algorithms shows itself in the concrete global results which are difficult to obtain by previous methods. This global approach is shown to shed new light on the qualitative methods now popular in dynamical systems theory.

In this paper we have only hinted at the possible applications. The examples have been chosen for their illustrative properties. In a sequel to this paper we shall focus our attention on one particular attractive sphere of application. That is, the analysis, and qualitative validation of nonlinear models constructed using system identification techniques.

Acknowledgment

The authors gratefully acknowledge that this work has been supported by the SERC.

References

BRINDLEY J., C. KASS-PETERSON, A. SPENCE, 1989, Path following methods in bifurcation problems, *Physica D*, **34**, 456-61.

DOEDEL E.J., 1981, AUTO - A program for the automatic bifurcation analysis of autonomous systems, *Congress. Numer.*, **30**, 265-84.

DOEDEL E.J., 1986, AUTO - Software for continuation and bifurcation probles in ordinary differential equations, (Calif. Inst. Tech.: USA).

GUMOWSKI I., C. MIRA, 1980, Recurences and Discete Dynamical Systems, *Lect. Notes Math.*, **809**, (Springer Verlag: Berlin).

HAHN H., 1985, Computation of branching solutions for a nonlinear control system via dual input describing function and root locus techniques, *Int. J. Control*, **42**, 21-31.

HASSARD B., N.D. KAZARINOFF, Y.H. WAN, 1980, Theory and Application of the Hopf Bifurcation, *London Math. Soc. Lect. Notes Series*, **41**, (Cambridge Univ. Press: Cambridge UK).

HENTE A., R.H. JANSEN, 1986, Frequency domain continuation methods for the analysis and stability investigation of nonlinear microwave circuits, *IEE Proc., part H*, **133**, 351-362.

HSU C.S., 1980e, A theory of cell-to-cell mapping dynamical systems, *Trans. ASME J. Appl. Mech.*, **47**, 931-39.

HSU C.S., 1981, A generalised theory of cell-to-cell mappings for nonlinear dynamical systems, *J. Appl. Mech.*, **48**, 634-42.

HSU C.S., 1982, A probabalistic theory of nonlinear dynamical systems based on the cell state space concept, *Trans. ASME J. Appl. Mech.*, **49**, 895-902.

HSU C.S., 1983, Singularities of n-dimensional cell functions and the associated index theory, *Int. J. Nonlinear Mech.*, **18**, 199-221.

HSU C.S., 1985a, Domains of attraction for multiple cycles of coupled Van der Pol Equations by simple cell mapping, *Int. J. Nonlinear Mech.*, **20**, 507-17.

HSU C.S., 1987, Cell-to-Cell Mapping: A method for the global analysis of nonlinear systems, *Appl. Math. Sci.*, **64**, (Springer Verlag: New York, Berlin).

HSU C.S., A. POLCHAI, 1984, Characteristics of singular entities of simple cell mappings, *Int. J. Nonlinear Mech.*, **19**, 19-38.

HSU C.S., R.S. GUTTALU, 1980, An unravelling algorithm for the global analysis of dynamical systems. An application of cell-to-cell mappings, *Trans. ASME J. Appl. Mech.*, **47**, 940-48.

HSU C.S., R.S. GUTTALU, W.H. ZHU, 1982, A method of analysing generalised cell mappings, *Trans. ASME J. Appl. Mech.*, **49**, 885-94.

HSU C.S., W.H. LEUNG, 1984, Singular entities and an index theory for cell functions, *J Math. Anal. Appl.*, **100**, 250-91.

KASS-PETERSEN C., 1987a, Continuation methods as a link between perturbation analysis and asymptotic analysis, *SIAM Rev.*, **29**, 115-20.

KASS-PETERSEN C., 1987b, PATH - User's guide, Centre for Nonlinear Studies and Dept. Appl. Math. Studies, (University of Leeds: Leeds, UK).

KELLER H.B., 1977, Numerical solution of bifurcation and nonlinear eigenvalue problems, in, *Application of Bifurcation Theory, Proceeding Seminar, Math. Res. Center, Univ. Wisconsin*, (Academic Press: New York, London).

KUBICEK M., 1976, ALGORITHM 502, Dependence of the solution of nonlinear systems on a parameter, *ACM-TOMS*, **2**, 98-107.

MARSDEN J., M. MACRACKEN, 1976, The Hopf Bifurcation and its Applications, *Appl. Math. Sci.*, (Springer Verlag: New York, Berlin).

MITTLEMANN H.D., 1986, A pseudo-arclength continuation method for nonlinear eigenvalue problems, *SIAM J. Numer. Anal.*, **23**, 1007-16.

RHEINBOLDT W.C., 1978, Numerical method for a class of finite dimensional bifurcation problems, *SIAM J. Numer.*

Anal., **15**, 1-11.

RHEINBOLDT W.C., 1986, Numerical Analysis of Parameterised Nonlinear Equations, (Wiley: New York).

RHEINBOLDT W.C., 1988, On the computation of multidimensional solution manifolds of parameterised equations, *Numer. Math.*, **53**, 165-81.

RHEINBOLDT W.C., J.V. BURKARDT, 1983, Algorithm 596: PITCON. A program for a locally parameterised continuation process, *ACM-TOMS*, **9**, 215-41.

ROOSE D., 1987, Numerical computation of origins of Hopf Bifurcation in a two parameter problem, in, *Bifurcation Analysis, Algorithms, Applications*, Report ISNM 79, [Ed] T. KUPPER, R. SEYDEL AND H. TROGER, 268-76, (Birkhauser: Basel).

ROOSE D., B. DEIR, 1987, Numerical determination of an emanating branch of Hopf Bifurcation points in a two parameter problem, Report TW-82: Dept. Comput. Sci. , (K.U. Leuven, Belgium).

SEYDEL R., 1979a, Dissertation, Math. Institute TU Munich, 1977 (part published.), *Numer. Math.*, **32**, 51-68.

SEYDEL R., 1979b, Numerical computation of branch points in nonlinear equations, *Numer. Math.*, **33**, 339-52.

SEYDEL R., 1983a, Branch switching in bifurcation problems for ODE's, *Numer. Math.*, **41**, 93-116.

SEYDEL R., 1983b, BIFPACK, *Appl. Math. Comput*, **9**, 257-71.

THOMPSON J.M.T., H.B. STEWART, 1986, Nonlinear Dynamics and Chaos, *Geometric methods for Engineers and Scientists*, (Wiley: UK).

WOOD E.F., J.A. KEMPF, R.K. MEHRA, 1984, BISTAB: A portable bifurcation and stability analysis package, *Appl. Math. Comp.*, **15**, 343-55.

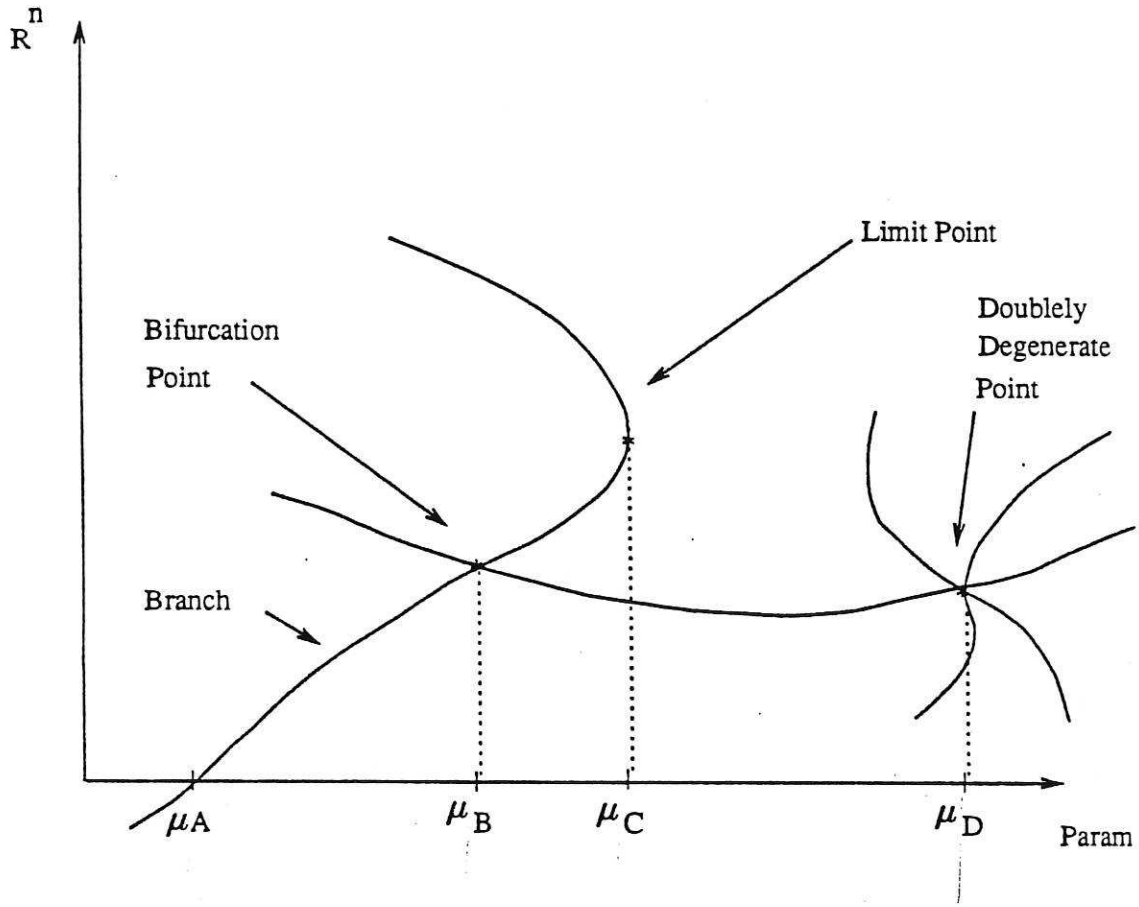

Fig. 0 Typical solution branch structure.

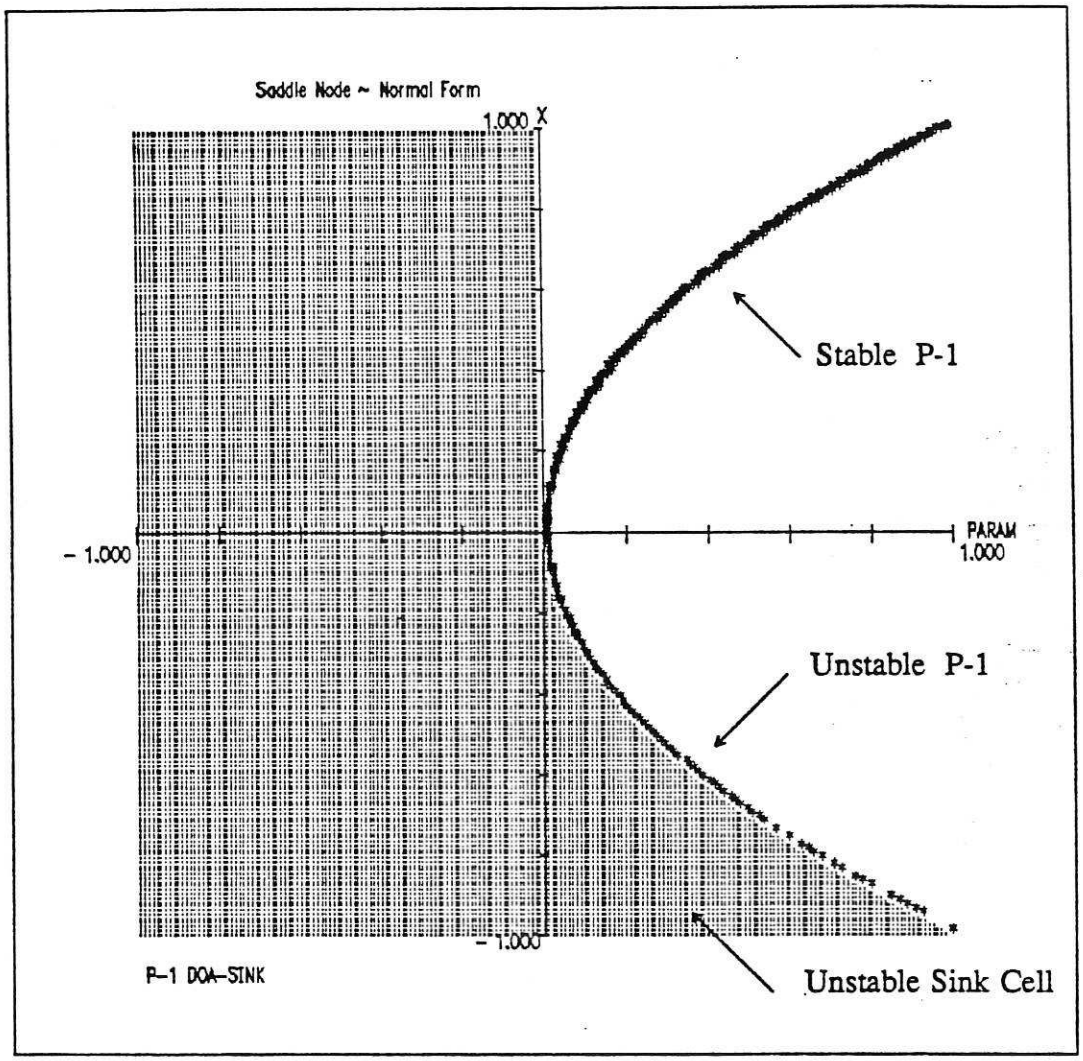

Fig. 1 CELL Diagram ~ Saddle Node ~ Normal Form

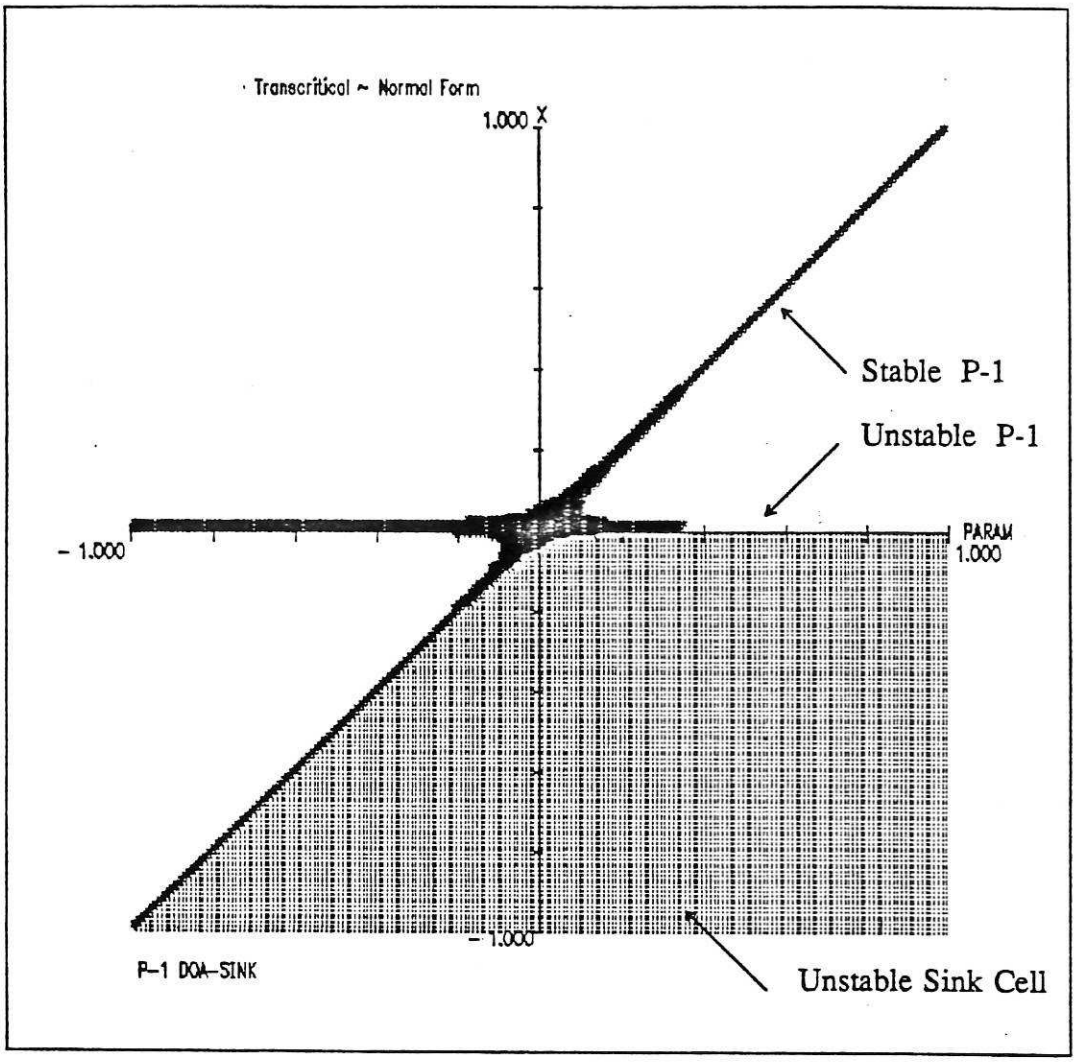

Fig. 2 CELL Diagram ~ Transcritical ~ Normal Form

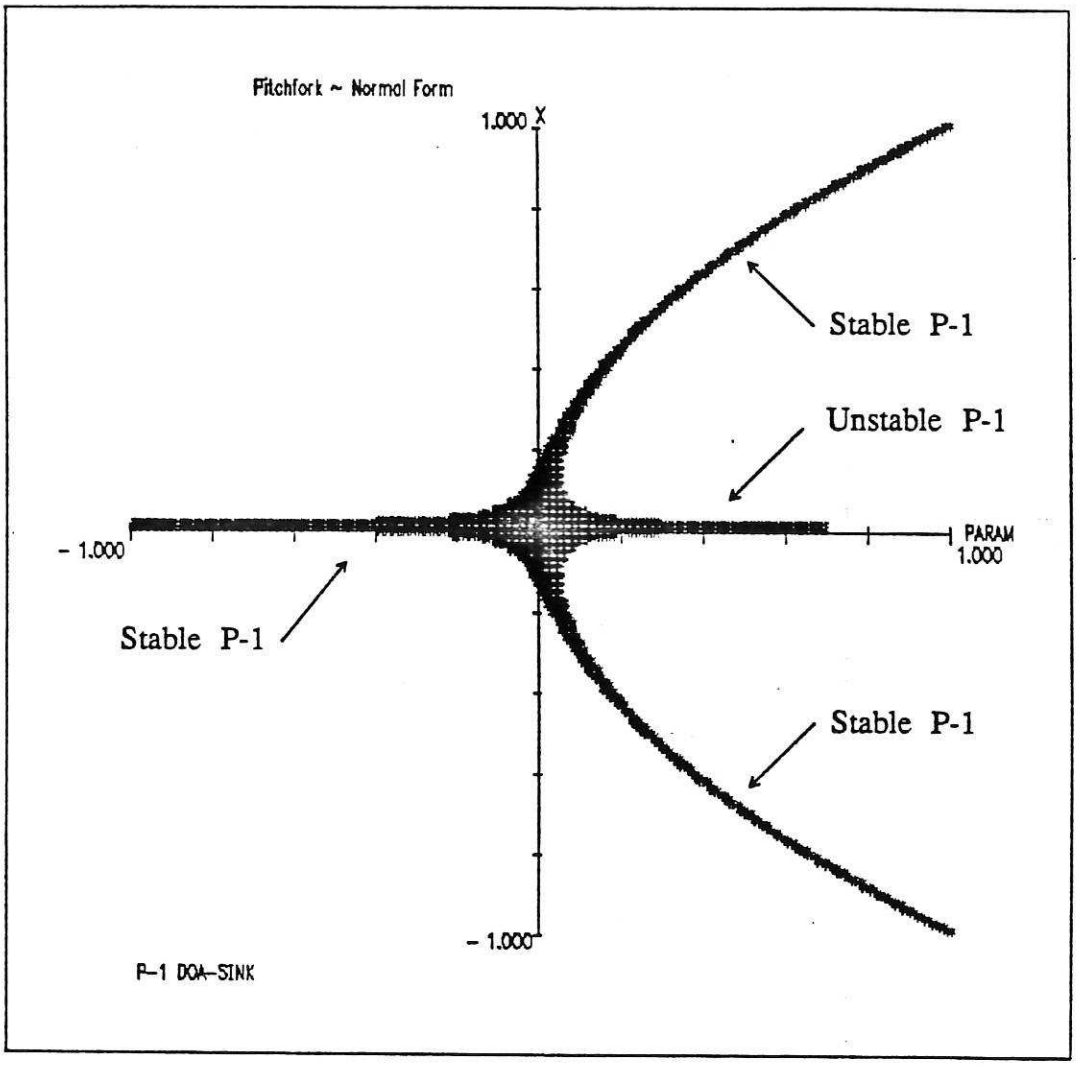

Fig. 3 CELL Diagram ~ Pitchfork ~ Normal Form

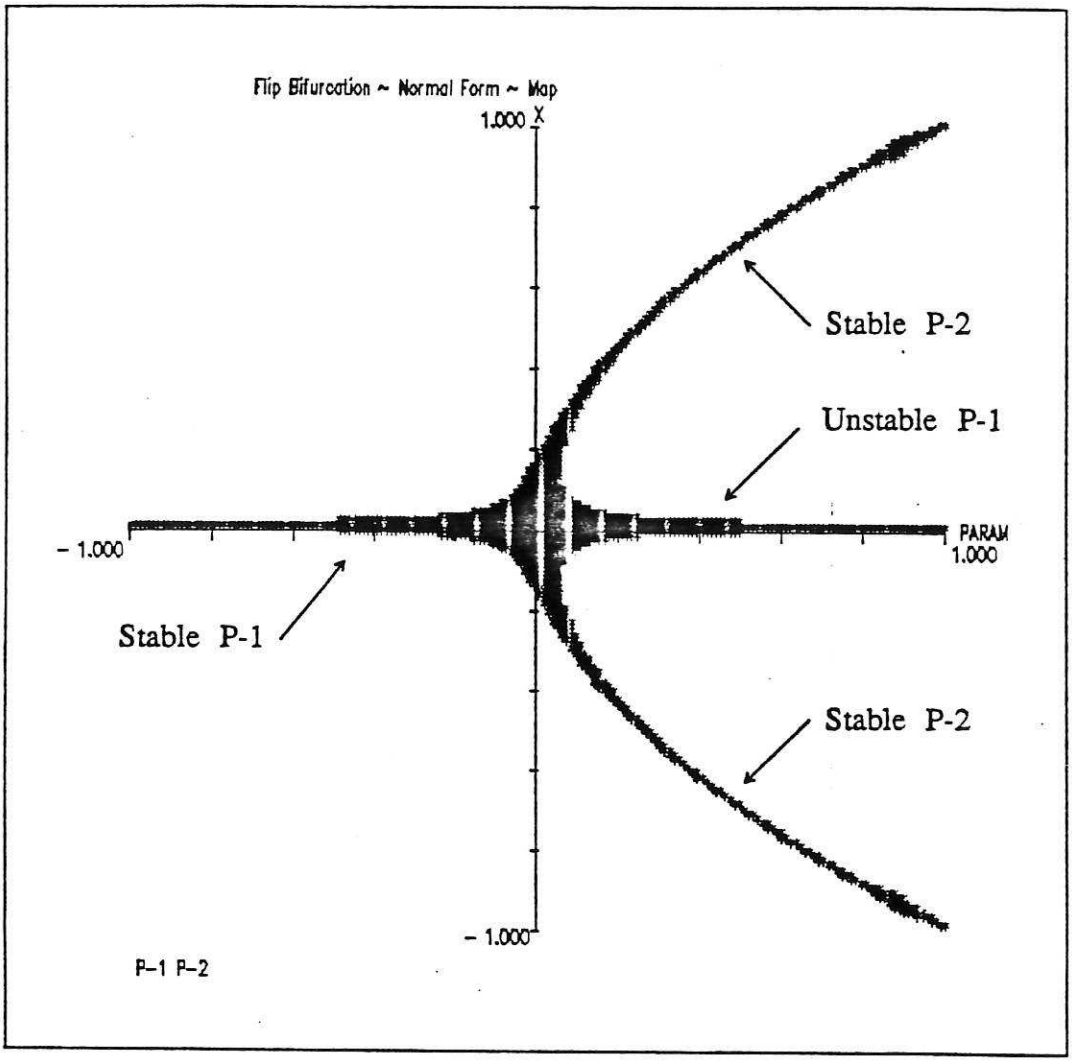

Fig. 4 CELL Diagram ˜ Flip Bifurcation ˜ Normal Form

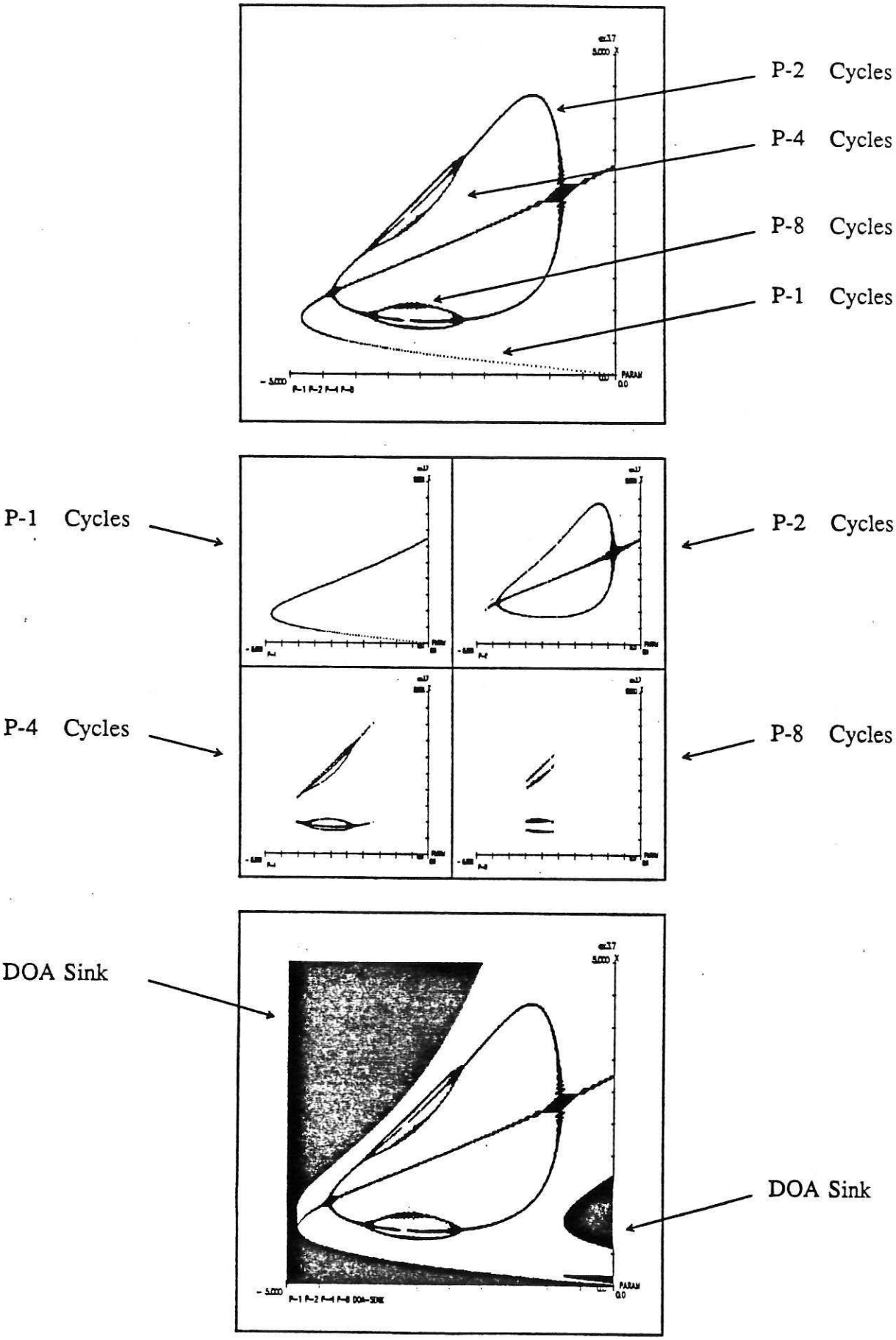

Fig. 5 CELL Diagram - Incomplete Cascade to Chaos

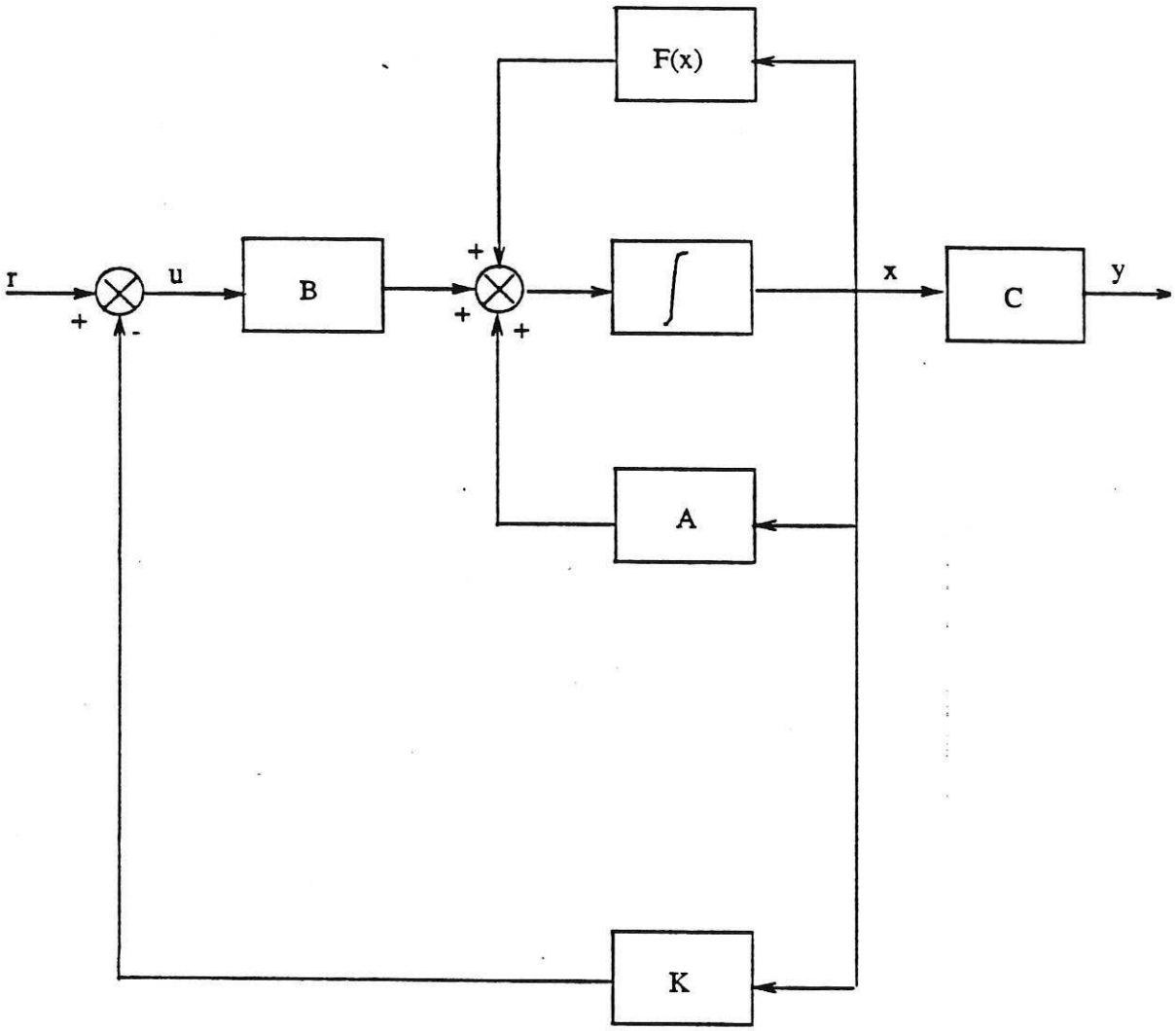

Fig. 6a Hahn Nonlinear Feedback System Block Diagram

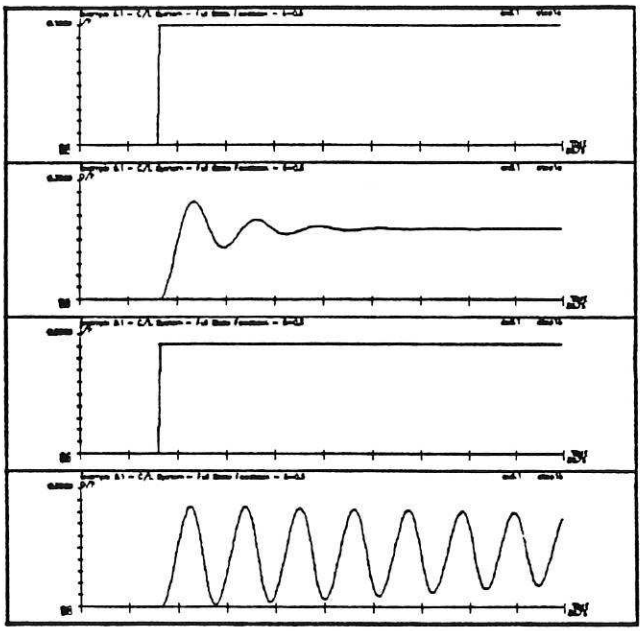

k = 0.5

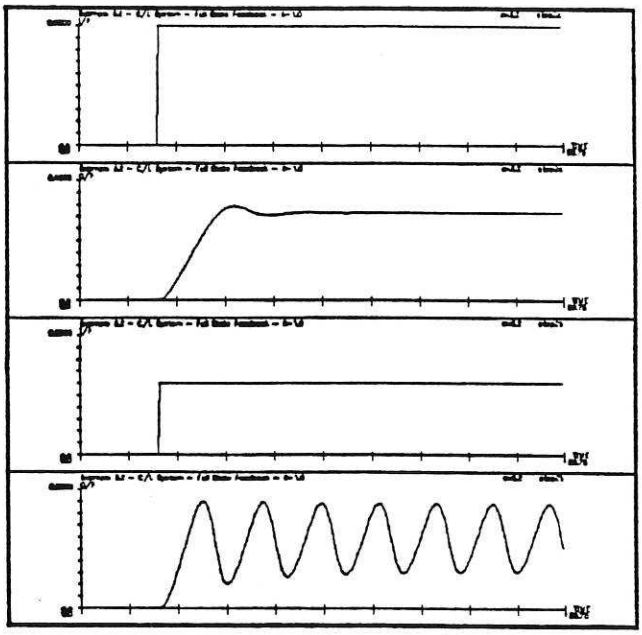

k = 1.0

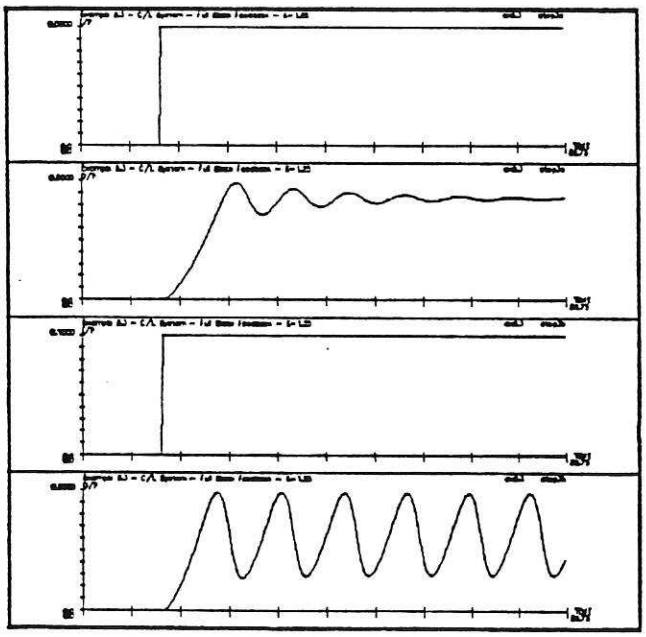

k = 1.25

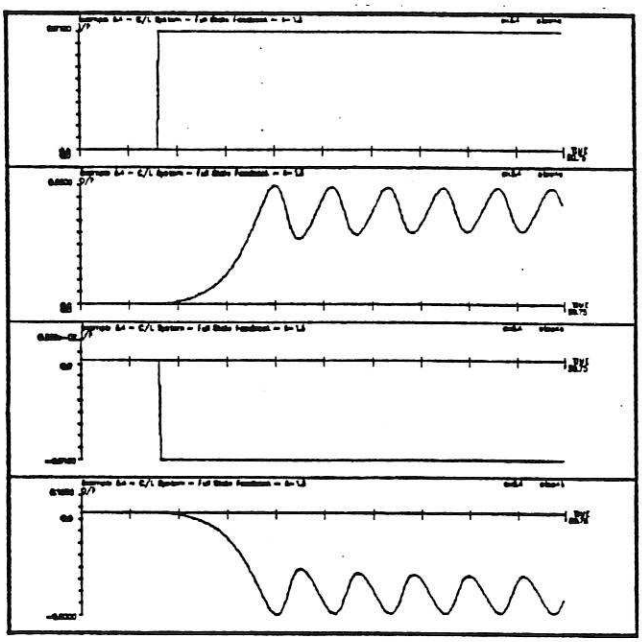

k = 1.5

Fig. 6b Step data, $k = 0.5$, $k = 1.0$, $k = 1.25$ and $k = 1.5$

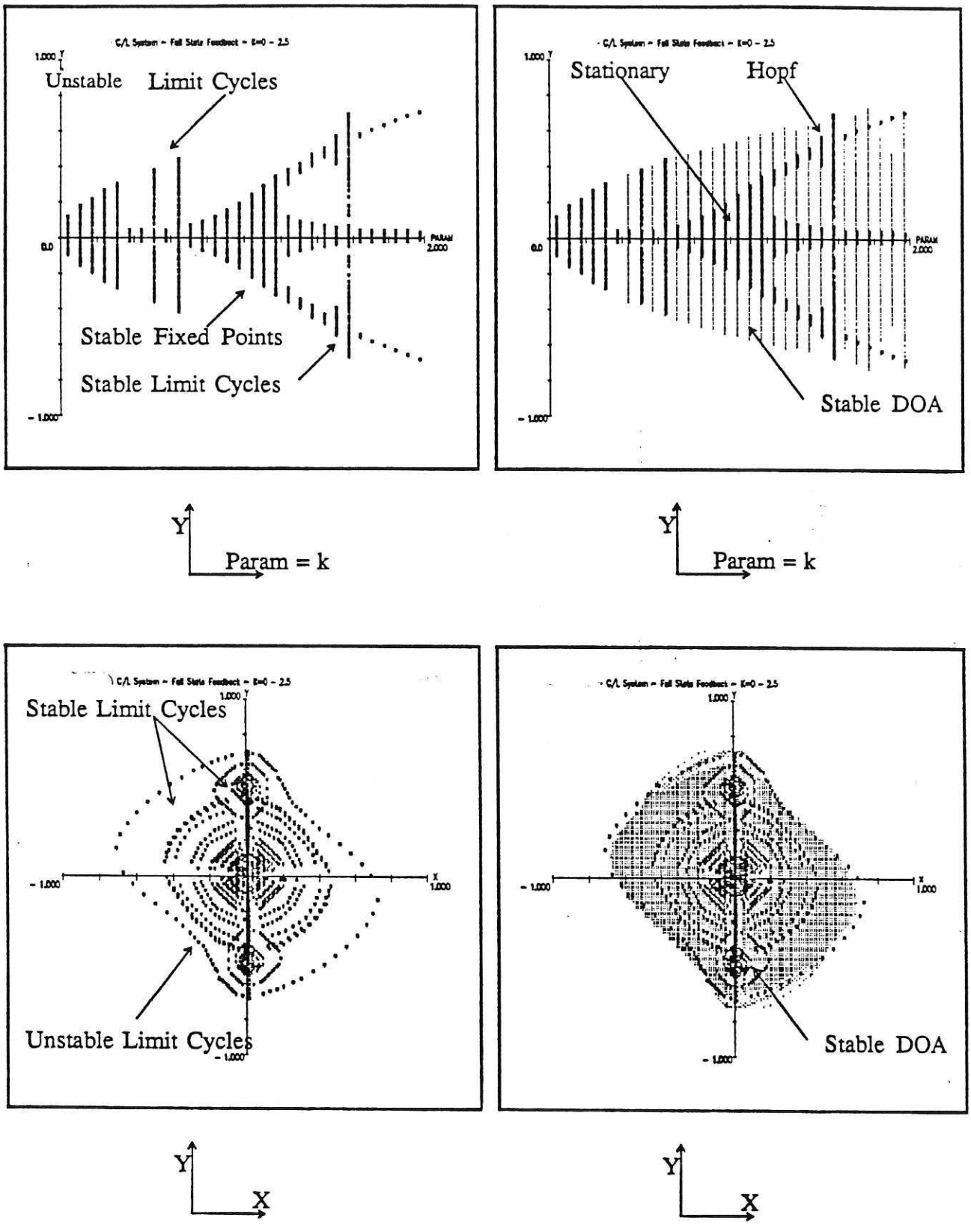

Fig. 6c **CELL** Diagram, $\mu = k\,r = 0.0$

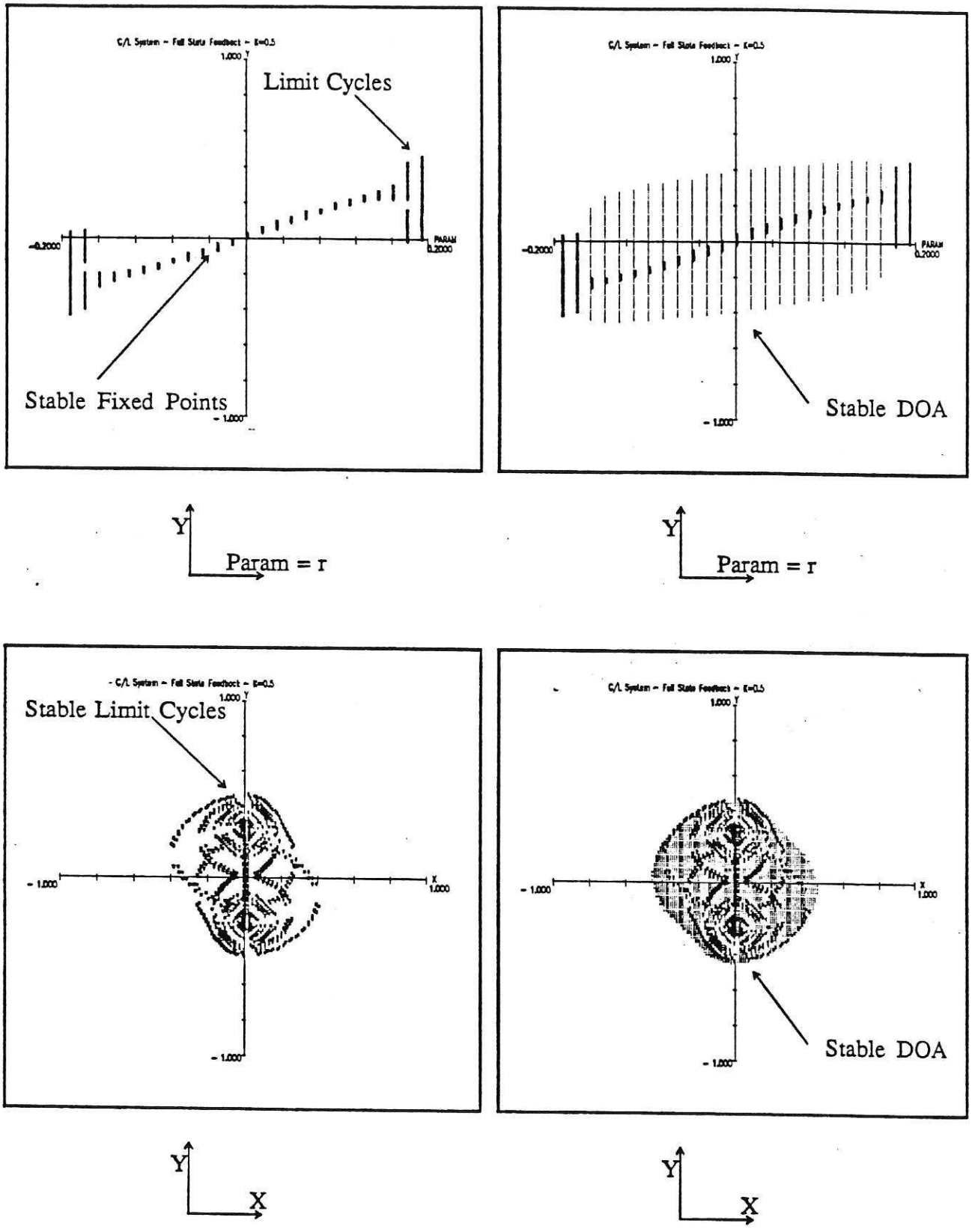

Fig. 6d **CELL** Diagram, $\mu = r$, $k = 0.5$

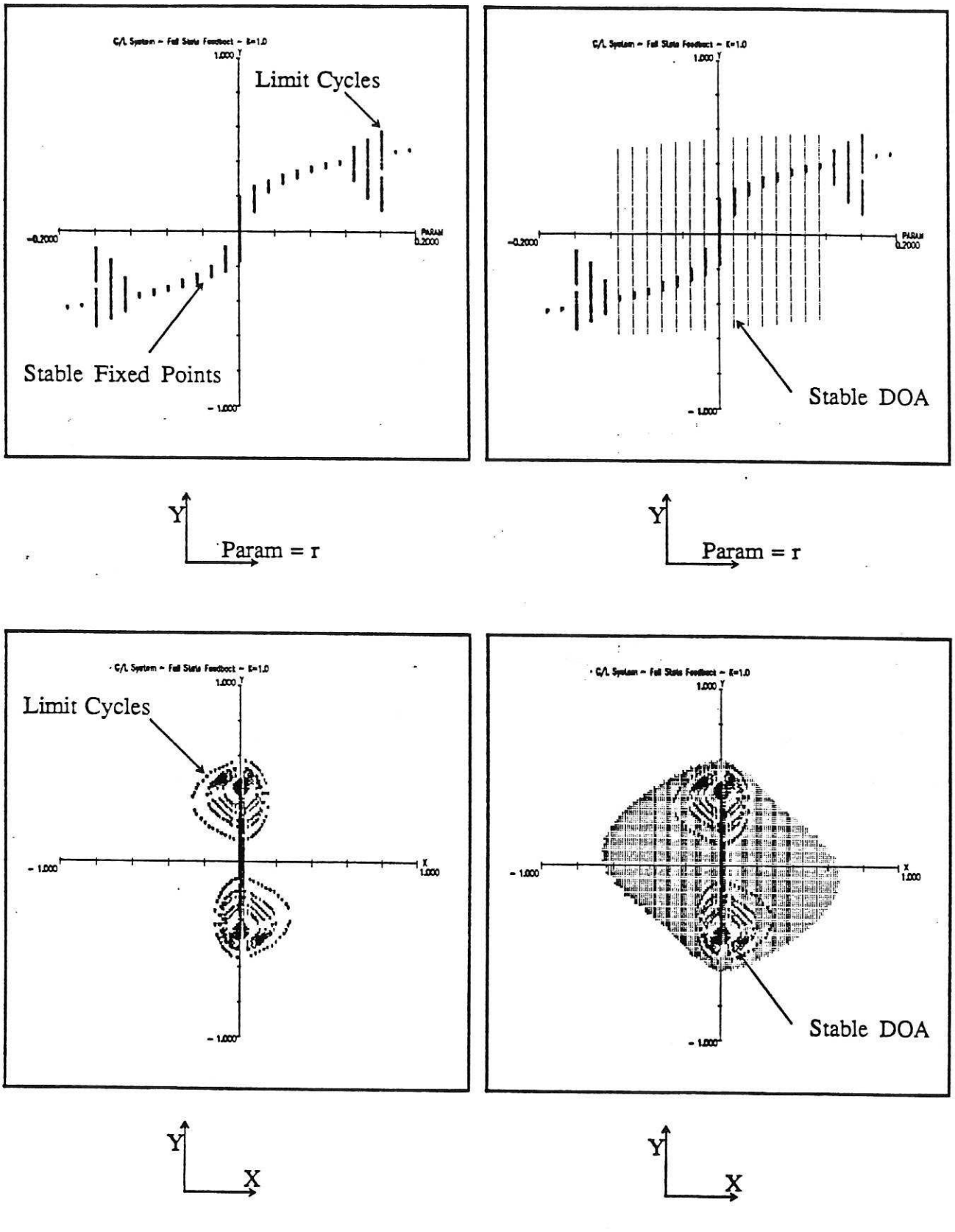

Fig. 6e CELL Diagram, $\mu = r$, $k = 1.0$

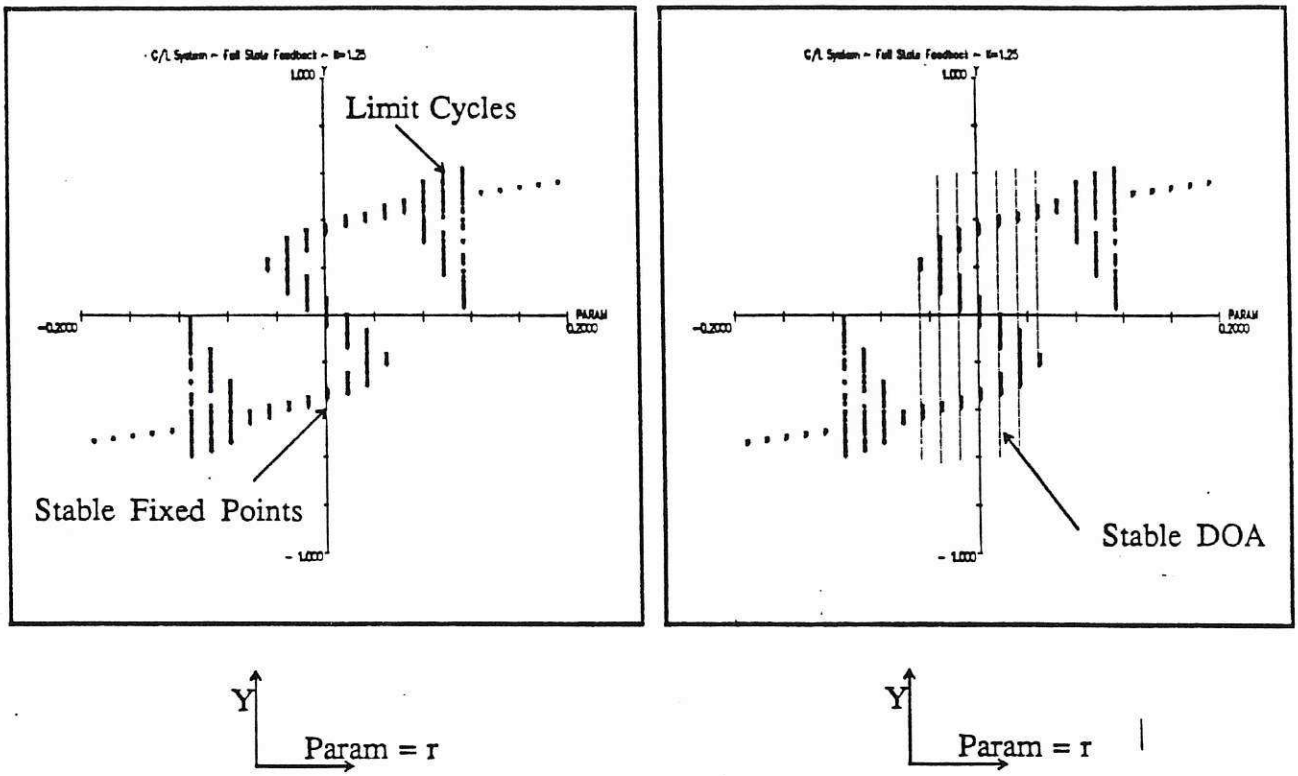

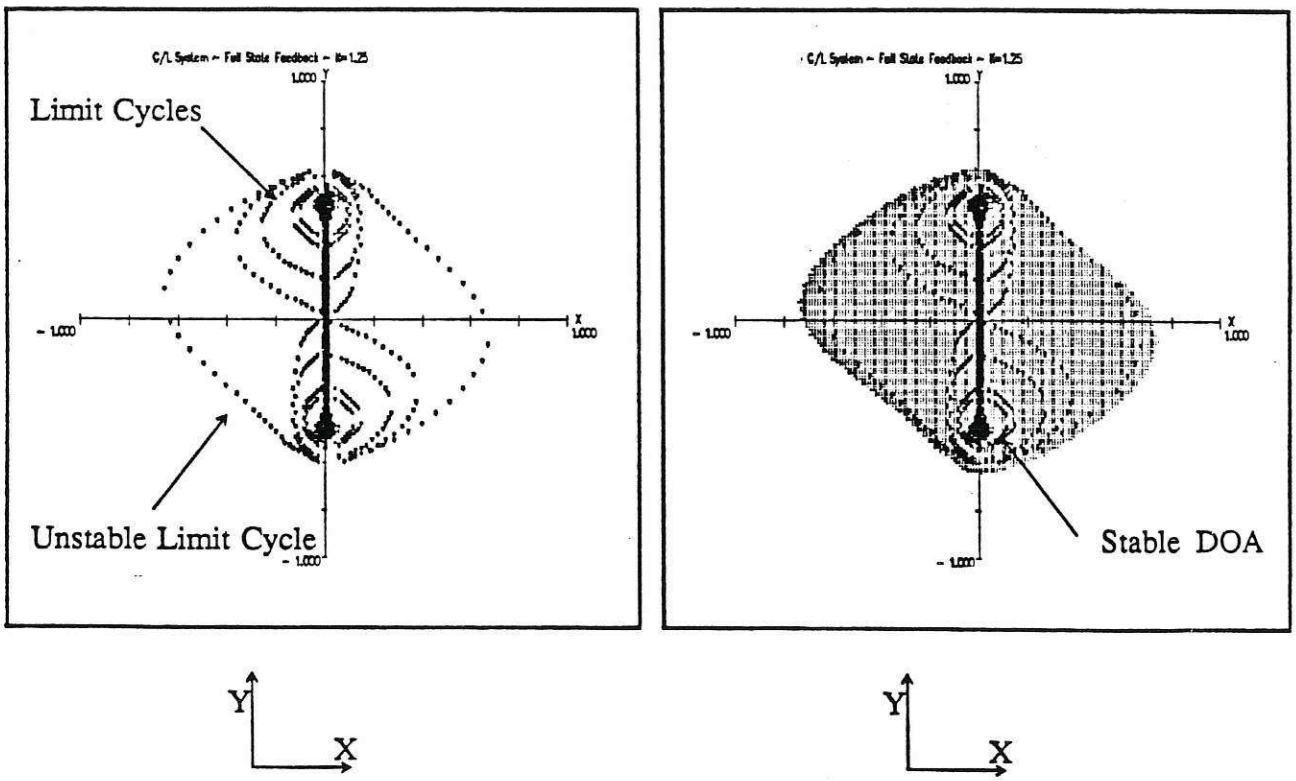

Fig. 6f **CELL** Diagram, $\mu = r$, $k = 1.25$